一般社団法人 電子情報通信学会
THE INSTITUTE OF ELECTRONICS,
INFORMATION AND COMMUNICATION ENGINEERS

信学技報
IEICE Technical Report

Impact of Channel Estimation Error on Analog SC-FDE using STTD Combined with Receive Antenna Diversity

Thanh Hai VO † Shinya KUMAGAI † and Fumiyuki ADACHI ‡

† ‡ Department of Communications Engineering, Graduate School of Engineering, Tohoku University
6-6-05 Aza-Aoba, Aramaki, Aoba-ku, Sendai-shi, Miyagi, 980-8579 Japan
E-mail: † {vothanhhai, kumagai}@mobile.ecei.tohoku.ac.jp, ‡ adachi@ecei.tohoku.ac.jp

Abstract In order to improve performance of analog signal transmission, we recently proposed a novel analog single-carrier transmission with frequency-domain equalization (analog SC-FDE). Additionally, we showed that a joint use of space-time transmit diversity (STTD) and receive antenna diversity significantly improves performance of our proposed analog SC-FDE under a perfect knowledge of channel state information at the receiver. In this paper, the well-known cyclic delay pilot channel estimation (CDP-CE) is considered and the impact of channel estimation error is studied for an application of analog SC-FDE to, as an example, radio broadcasting. It is shown, by computer simulation, that CDP-CE keeps the normalized mean square error (NMSE) performance similar to that under the perfect knowledge of channel state information even in a very high mobility environment.

Keyword Analog signal transmission, Frequency-domain equalization, Single-carrier transmission, STTD, Receive antenna diversity, Cyclic delay pilot, Channel estimation

1. Introduction

Nowadays, although digital signal transmission has been continuously evolving [1]-[2], analog signal transmission (e.g., radio broadcasting) still remains essential. The signal bandwidth of analog signal transmission is much narrower than that of digital signal transmission since neither source coding nor channel coding is used. In other words, analog signal transmission has much higher spectrum efficiency. The propagation channel for analog signal transmission is a frequency-nonselective fading channel [3]. Consequently, the received signal power drops over a consecutive period of time with high probability and hence, the received signal quality seriously degrades. In order to overcome this problem, we recently proposed a new analog signal transmission technique that is referred to as analog single-carrier transmission with frequency-domain equalization (analog SC-FDE) [4]. Analog SC-FDE applies discrete Fourier transform (DFT), frequency-domain spectrum shaping and mapping, inverse DFT (IDFT), and cyclic prefix (CP) insertion before transmission. At the receiver, one-tap frequency-domain equalization (FDE) [5]-[6] is applied to take advantage of frequency-selective fading channel. The normalized mean square error (NMSE) is used to evaluate the transmission performance of proposed analog SC-FDE. We showed that it achieves better NMSE performance than that of conventional analog signal transmission [4].

In order to further improve the transmission performance of analog SC-FDE, a combination of STTD and receive antenna diversity can be used. We showed that analog SC-FDE using STTD combined with receive antenna diversity [7] significantly improves NMSE performance of our proposed analog SC-FDE under a perfect knowledge of channel state information (CSI) at the receiver. However, any practical channel estimation causes channel estimation error. Therefore, it is practically important to examine an impact of the channel estimation error on NMSE performance. One of the well-known channel estimation schemes for multiple-input multiple-output (MIMO) systems is the cyclic delay pilot channel estimation (CDP-CE) [8]. In CDP-CE, each transmit antenna uses pilot blocks having different cyclic delays generated from a known pilot block. All antennas simultaneously transmit the pilot blocks for a simultaneous channel gain estimation of all transmit and receive antenna pairs.

In this paper, we study the impact of channel estimation error of CDP-CE under a doubly selective (i.e., time-varying and frequency-selective) Rayleigh fading channel for an application of analog SC-FDE to, as an example, radio broadcasting. The remainder of this paper is organized as follows. In Section 2, analog SC-FDE using STTD combined with receive antenna diversity under CDP-CE is presented. Simulation results are given in Section 3. Finally, Section 4 provides conclusion.

2. Analog SC-FDE using STTD Combined with Receive Antenna Diversity

2.1. System Model

STTD based on space-time block code (STBC) has been well studied in [9]-[10]. An extended work on STTD

combined with receive antenna diversity for SC-FDE is found in [11]. STTD combined with receive antenna diversity can also be applied to analog SC-FDE.

System model of analog SC-FDE using STTD combined with receive antenna diversity under CDP-CE is illustrated in Fig. 1. At the transmitter having N_t transmit antennas, after the signal bandwidth is limited by low-pass filter (LPF), the analog signal $s(t)$ to be transmitted is sampled at the Nyquist rate. Then, the sample sequence is grouped into a sequence of signal blocks of M samples each. Each signal block $\{s(n);\ n=0\sim M-1\}$ is transformed by M-point DFT into frequency-domain signal block. Spectrum shaping filter is introduced in order to generalize the proposed system model having a specific spectrum shaping design. Then, STBC encoding is implemented to obtain N_t parallel streams of encoded signal blocks. The resultant M frequency components, which are referred to as M subcarriers, of each encoded block are mapped over a broad bandwidth having N_c ($>M$) orthogonal subcarriers with zeros occupying the unused subcarriers. Then, each encoded block of N_c subcarriers is transformed back into complex time-domain signal block $\{x_{q,n_t}(n);\ n=0\sim N_c-1\}$ by N_c-point IDFT. Finally, the last N_g samples of each transmission block are copied as a CP and inserted into the guard interval (GI) placed at the beginning of each data block. For channel estimation at the receiver, each transmit antenna uses the pilot block having different cyclic delays generated from a known pilot block of N_p samples. The pilot blocks were also inserted CP before being added to the beginning of the data blocks for simultaneous transmission.

The pilot-added signal blocks are simultaneously transmitted from N_t antennas over a doubly selective Rayleigh fading channel. N_r receive antennas are used at the receiver. First, the pilot blocks are separated from data blocks for channel estimation. The frequency-domain channel gains are estimated from pilot blocks by applying removal of CP, N_p-point DFT, composite channel estimation, N_p-point IDFT, windowing, delay-time shift and N_c-point DFT. On the other hand, each data block after removing CP is transformed into the frequency-domain signal block by N_c-point DFT. De-mapping is then performed to pick up the desired M subcarriers before joint STBC decoding and one-tap MMSE-FDE, which uses the estimated channel gains, is applied to obtain frequency diversity gain. Then, each M-subcarrier block is transformed back into complex time-domain signal $\{\tilde{s}(n);\ n=0\sim M-1\}$. Real part of the signal is outputted and finally, the analog signal $\tilde{s}(t)$ is reconstructed by automatic gain control (AGC) [12] and LPF.

2.2. Transmit Signal

At the transmitter, we assume that spectrum shaping filter is an ideal brick wall LPF. After applying DFT and spectrum shaping filter, J blocks of M subcarriers are grouped $\{S_j(k);\ k=0\sim M-1,\ j=0\sim J-1\}$ and expressed as

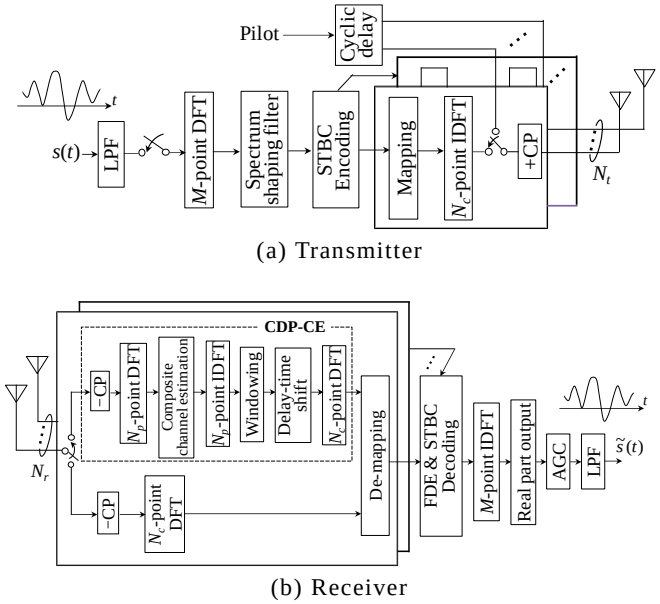

Fig. 1. System model.

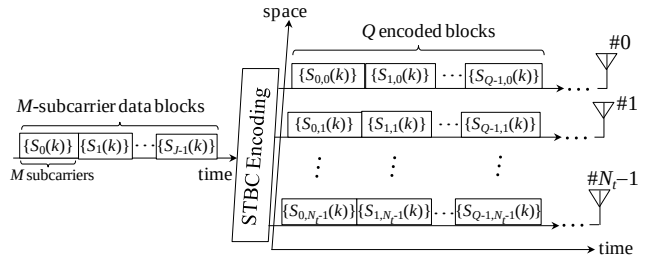

Fig. 2. STBC encoding.

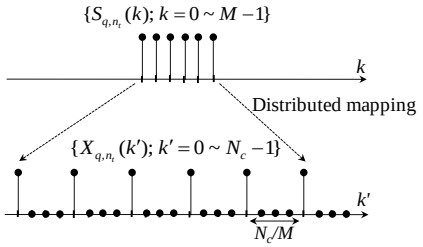

Fig. 3. Subcarrier mapping.

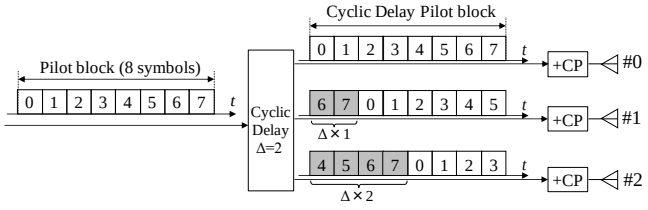

Fig. 4. Generation of cyclic delay pilot.

$$S_j(k)=\frac{1}{\sqrt{M}}\sum_{n=0}^{M-1}s_j(n)\exp\left(-j2\pi k\frac{n}{M}\right). \quad (1)$$

Then, the grouped J blocks are encoded by STBC encoding into N_t parallel streams of Q encoded blocks $\{S_{q,n_t}(k);\ k=0\sim M-1,\ q=0\sim Q-1,\ n_t=0\sim N_t-1\}$ as shown in Fig. 2. The k-th frequency component of N_t parallel

streams of Q encoded blocks is represented as $N_t \times Q$ space-time encoding matrix $\mathbf{S}_{N_t} = [\mathbf{S}_0(k),..., \mathbf{S}_q(k),..., \mathbf{S}_{Q-1}(k)]$, where $\mathbf{S}_q(k) = [S_{q,0}(k),..., S_{q,n_t}(k),..., S_{q,N_t-1}(k)]^T$ is the q-th encoded frequency-domain signal vector and $[.]^T$ denotes the transpose operation. As $\mathbf{S}_{N_t}(k)$, the following space-time encoding matrices [9]-[10] are used.

$$\mathbf{S}_{N_t=1}(k) = S_0(k), \tag{2.a}$$

$$\mathbf{S}_{N_t=2}(k) = \frac{1}{\sqrt{2}}\begin{bmatrix} S_0(k) & -S_1^*(k) \\ S_1(k) & S_0^*(k) \end{bmatrix}, \tag{2.b}$$

$$\mathbf{S}_{N_t=3}(k) = \frac{1}{\sqrt{3}}\begin{bmatrix} S_0(k) & -S_1^*(k) & -S_2^*(k) & 0 \\ S_1(k) & S_0^*(k) & 0 & -S_2^*(k) \\ S_2(k) & 0 & S_0^*(k) & S_1^*(k) \end{bmatrix}, \tag{2.c}$$

$$\mathbf{S}_{N_t=4}(k) = \frac{1}{\sqrt{4}}\begin{bmatrix} S_0(k) & -S_1^*(k) & -S_2^*(k) & 0 \\ S_1(k) & S_0^*(k) & 0 & -S_2^*(k) \\ S_2(k) & 0 & S_0^*(k) & S_1^*(k) \\ 0 & S_2(k) & -S_1(k) & S_0(k) \end{bmatrix}, \tag{2.d}$$

where $[.]^*$ denotes the complex conjugate operation.

For each encoded data block, distributed mapping [14] is adopted in order to take advantage of the channel frequency selectivity (i.e., frequency diversity gain) [4]. M subcarriers of each encoded block $\{S_{q,n_t}(k);\ k=0\sim M-1\}$ are mapped with equally-spaced intervals over a broad bandwidth having N_c ($>M$) orthogonal subcarriers expressed as $\{X_{q,n_t}(k');\ k'=0\sim N_c-1\}$ in Eq. (3) in which zero occupies the unused subcarriers. An example of subcarrier mapping with M = 6, N_c = 24 is illustrated in Fig. 3.

$$X_{q,n_t}(k') = \begin{cases} S_{q,n_t}(k) & ,\ k' = k \times \dfrac{N_c}{M} \\ 0 & ,\ \text{otherwise} \end{cases}, \tag{3}$$

where $k=0\sim M-1$, $k'=0\sim N_c-1$, $q=0\sim Q-1$, $n_t=0\sim N_t-1$ and N_c/M is the adjacent subcarrier interval. After N_c-point IDFT, the time-domain sample sequence at a rate of $1/T_s=(N_c/M)\times 1/T$, in which $1/T$ is the Nyquist sampling rate of analog signal $s(t)$, is obtained. The CP-inserted time-domain sample sequence $\{\tilde{x}_{q,n_t}(n);\ n=-N_g\sim N_c-1\}$ can be expressed using the equivalent low-pass representation as

$$\tilde{x}_{q,n_t}(n) = \sqrt{2P}\, x_{q,n_t}(n \bmod N_c), \tag{4}$$

where P is the average sample sequence power and $\{x_{q,n_t}(n);\ n=0\sim N_c-1\}$ is given by

$$x_{q,n_t}(n) = \frac{1}{\sqrt{N_c}} \sum_{k=0}^{N_c-1} X_{q,n_t}(k) \exp\left(j2\pi n \frac{k}{N_c} \right). \tag{5}$$

2.3. Cyclic Delay Pilot Transmission

In CDP-CE, a known pilot block $\{p(n);\ n=0\sim N_p-1\}$ is used to generate different cyclic delay pilots $\{p_{n_t}(n);\ n=0\sim N_p-1,\ n_t=0\sim N_t-1\}$ for N_t transmit antennas expressed as [8]

$$p_{n_t}(n) = p\left((n - \Delta \cdot n_t) \bmod N_p\right), \tag{6}$$

where Δ is the unit cyclic delay $(N_g \le \Delta \le N_p / N_t)$. An example of N_p = 8 and N_t = 3 is shown in Fig. 4. In frequency domain, the representation of cyclic delay pilot $\{P_{n_t}(k);\ k=0\sim N_p-1,\ n_t=0\sim N_t-1\}$ is given by

$$P_{n_t}(k) = P(k) \exp\left(-j2\pi k \frac{\Delta n_t}{N_p} \right), \tag{7}$$

where $P(k)$ is the k-th frequency component of the original pilot block $\{p(n);\ n=0\sim N_p-1\}$.

After CP insertion, cyclic delay pilot blocks $\{\tilde{p}_{n_t}(n);\ n=-N_g\sim N_p-1,\ n_t=0\sim N_t-1\}$ are added to the beginning of the data block and simultaneously transmitted from N_t transmit antennas. The CP-inserted time-domain pilot block $\{\tilde{p}_{n_t}(n);\ n=-N_g\sim N_p-1\}$ can be expressed using the equivalent low-pass representation as

$$\tilde{p}_{n_t}(n) = \sqrt{2P}\, p_{n_t}(n \bmod N_p). \tag{8}$$

2.4. Received Signal

Assuming that the channel consists of L distinct propagation paths, the channel impulse response $h_{n_r,n_t}(\tau,n)$ can be expressed as

$$h_{n_r,n_t}(\tau,n) = \sum_{l=0}^{L-1} h_{n_r,n_t,l}(n)\delta(\tau - \tau_{n_r,n_t,l}), \tag{9}$$

where $h_{n_r,n_t,l}(n)$, $\tau_{n_r,n_t,l}$, and $\delta(.)$ are complex-valued path gain with $E[\sum_{l=0}^{L-1}|h_{n_r,n_t,l}(n)|^2]=1$ ($E[.]$ denotes ensemble average operation), sample-spaced time delay of the l-th path (i.e., $\tau_{n_r,n_t,l} = l$), and delta function, respectively. It is assumed that the maximum time delay of channel is shorter than the CP size and the received signal is ideally sampled at the rate $1/T_s$.

At the receiver, the superposition of N_t transmitted signals is received by N_r receive antennas. Pilot blocks and data blocks are separated as shown in Fig. 1(b) for different signal processing which are described in Sections 2.4.1 and 2.4.2, respectively.

2.4.1. Cyclic Delay Pilot Channel Estimation

The discrete-time received pilot signal $\{r_{p,n_r}(n);\ n=-N_g\sim N_p-1,\ n_r=0\sim N_r-1\}$ at n_r-th receive antenna is expressed as

$$\begin{aligned} r_{p,n_r}(n) &= \sum_{n_t=0}^{N_t-1}\sum_{l=0}^{L-1} h_{n_r,n_t,l}(n)\tilde{p}_{n_t}(n-\tau_{n_r,n_t,l}) + \eta_{p,n_r}(n) \\ &\approx \sum_{n_t=0}^{N_t-1}\sum_{l=0}^{L-1} h_{n_r,n_t,l}\tilde{p}_{n_t}(n-\tau_{n_r,n_t,l}) + \eta_{p,n_r}(n) \end{aligned}, \tag{10}$$

where $\eta_{p,n_r}(n)$ is the additive white Gaussian noise (AWGN) with zero-mean and variance $2N_0/T_s$ in which N_0 is the single-sided power spectrum density. In Eq. (10), $h_{n_r,n_t,l}(n)$ is approximated by the average value $h_{n_r,n_t,l}$ of time-varying channel gain in the period of pilot block.

After removing CP, pilot signal block is transformed by N_p-point DFT into frequency-domain signal $\{R_{p,n_r}(k);\ k=0\sim N_p-1,\ n_r=0\sim N_r-1\}$ as

$$\begin{aligned} R_{p,n_r}(k) &= \sqrt{2P}\sum_{n_t=0}^{N_t-1} H_{n_r,n_t}(k)P_{n_t}(k) + \prod_{p,n_r}(k) \\ &= H'_{n_r}(k)P(k) + \prod_{p,n_r}(k), \end{aligned} \tag{11}$$

where $H_{n_r,n_t}(k)$, $\prod_{q,n_t}(k)$ and $H'_{n_r}(k)$ are respectively channel gain, noise and composite channel gain at the k-th frequency given by

$$H_{n_r,n_t}(k)=\sum_{l=0}^{L-1}h_{n_r,n_t,l}\exp\left(-j2\pi k\frac{\tau_{n_r,n_t,l}}{N_c}\right), \tag{12}$$

$$\prod_{p,n_r}(k)=\frac{1}{\sqrt{N_c}}\sum_{n=0}^{N_c-1}\eta_{p,n_r}(n)\exp\left(-j2\pi k\frac{n}{N_c}\right), \tag{13}$$

$$H'_{n_r}(k)=\sqrt{2P}\sum_{n_t=0}^{N_t-1}H_{n_r,n_t}(k)\exp\left(-j2\pi k\frac{\Delta n_t}{N_p}\right). \tag{14}$$

The estimation of the composite channel gain is next performed to obtain $\{\hat{H}'_{n_r}(k);\ k=0\sim N_p,\ n_r=0\sim N_r-1\}$ expressed as

$$\hat{H}'_{n_r}(k)=\frac{P^*_{n_t}(k)}{\left|P_{n_t}(k)\right|^2}R_{p,n_r}(k). \tag{15}$$

By applying N_p-point IDFT to Eq. (15), delay-time domain signal $\bar{h}_{n_r}(\tau)$ comprising channel impulse response and noise as shown in Fig. 5 is expressed as

$$\begin{aligned}\bar{h}_{n_r}(\tau)&=\frac{1}{\sqrt{N_p}}\sum_{k=0}^{N_p-1}\hat{H}'_{n_r}(k)\exp\left(j2\pi k\frac{\tau}{N_p}\right)\\&=\sqrt{2PN_p}\sum_{n_t=0}^{N_t-1}\sum_{l=0}^{L-1}h_{n_r,n_t,l}\delta(\tau-\tau_l-\Delta n_t)\\&\quad+\frac{1}{\sqrt{N_p}}\sum_{k=0}^{N_p-1}\frac{P^*_{n_t}(k)}{\left|P_{n_t}(k)\right|^2}\prod_{p,n_r}(k)\exp\left(j2\pi k\frac{\tau}{N_p}\right).\end{aligned} \tag{16}$$

Therefore, the estimated channel impulse response in delay-time domain $\bar{h}_{n_r,n_t}(\tau)=\{\bar{h}_{n_r,n_t,0},...,\bar{h}_{n_r,n_t,L-1}\}$ can be obtained after applying delay-time domain windowing and shift as

$$\bar{h}_{n_r,n_t}(\tau)=\begin{cases}\dfrac{1}{\sqrt{2PN_p}}\bar{h}_{n_r}(\tau+\Delta n_t) & ,\ if\ 0\le\tau<\Delta\\ 0 & ,\ \text{otherwise}\end{cases}. \tag{17}$$

Finally, frequency-domain channel gain $\{\bar{H}_{n_r,n_t}(k);\ k=0\sim N_c-1,\ n_r=0\sim N_r-1,\ n_t=0\sim N_t-1\}$ used for FDE is calculated by using N_c-point DFT as

$$\bar{H}_{n_r,n_t}(k)=\sum_{l=0}^{L-1}\bar{h}_{n_r,n_t,l}\exp\left(-j2\pi k\frac{\tau_{n_r,n_t,l}}{N_c}\right). \tag{18}$$

In addition to channel gain estimation, signal and noise power are also needed to estimate for calculating average received signal-to-noise power ratio (SNR) Γ [15]

$$\hat{\Gamma}=\frac{\left(N_p-\Delta N_t\right)\sum_{\tau=0}^{\Delta N_t-1}\left|\bar{h}_{n_r}(\tau)\right|^2\sum_{k=0}^{N_p-1}\frac{1}{\left|P(k)\right|^2}}{\left(N_p\right)^2N_t\sum_{\tau=\Delta N_t}^{N_p-1}\left|\bar{h}_{n_r}(\tau)\right|^2}. \tag{19}$$

2.4.2. Received Data Signal

The discrete-time received data signal $\{r_{q,n_r}(n);\ n=-N_g\sim N_c-1,\ q=0\sim Q-1,\ n_r=0\sim N_r-1\}$ at n_r-th receive antenna is expressed as

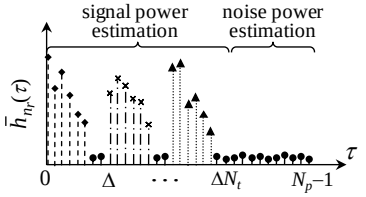

Fig. 5. Channel impulse response in delay-time domain.

$$\begin{aligned}r_{q,n_r}(n)&=\sum_{n_t=0}^{N_t-1}\sum_{l=0}^{L-1}h_{n_r,n_t,l}(n)\tilde{x}_{q,n_t}(n-\tau_{n_r,n_t,l})+\eta_{q,n_r}(n)\\&\approx\sum_{n_t=0}^{N_t-1}\sum_{l=0}^{L-1}h_{n_r,n_t,l}\tilde{x}_{q,n_t}(n-\tau_{n_r,n_t,l})+\eta_{q,n_r}(n)\end{aligned}, \tag{20}$$

where $\eta_{q,n_r}(n)$ is the AWGN with zero-mean and variance $2N_0/T_s$. In Eq. (20), $h_{n_r,n_t,l}(n)$ is approximated by the average value $h_{n_r,n_t,l}$ of time-varying channel gain in the period of Q encoded signal blocks.

After removing CP from data blocks, the receiver transforms each received signal block into the frequency-domain signal using N_c-point DFT. The frequency-domain received data signal at the k-th frequency $\{R_{q,n_r}(k);\ k=0\sim N_c-1,\ q=0\sim Q-1,\ n_r=0\sim N_r-1\}$ is expressed as

$$R_{q,n_r}(k)=\sqrt{2P}\sum_{n_t=0}^{N_t-1}H_{n_r,n_t}(k)X_{q,n_t}(k)+\prod_{q,n_r}(k), \tag{21}$$

where $\prod_{q,n_t}(k)$ is the noise component at the k-th frequency given by

$$\prod_{q,n_r}(k)=\frac{1}{\sqrt{N_c}}\sum_{n=0}^{N_c-1}\eta_{q,n_r}(n)\exp\left(-j2\pi k\frac{n}{N_c}\right). \tag{22}$$

De-mapping is then performed to obtain desired M frequency components $\{\hat{R}_{q,n_r}(k);\ k=0\sim M-1,\ q=0\sim Q-1,\ n_r=0\sim N_r-1\}$ of the encoded blocks. Channel gain $\{\hat{H}_{n_r,n_t}(k);\ k=0\sim M-1,\ n_t=0\sim N_t-1,\ n_r=0\sim N_r-1\}$ for FDE and the equivalent noise component $\{\hat{\prod}_{q,n_r}(k);\ k=0\sim M-1,\ q=0\sim Q-1,\ n_r=0\sim N_r-1\}$ are also obtained as

$$\begin{cases}\hat{R}_{q,n_r}(k)=R_{q,n_r}\left(k\times N_c/M\right)\\ \hat{H}_{n_r,n_t}(k)=\bar{H}_{n_r,n_t}\left(k\times N_c/M\right)\\ \hat{\prod}_{q,n_r}(k)=\prod_{q,n_r}\left(k\times N_c/M\right)\end{cases}, \tag{23}$$

where $\{\bar{H}_{n_r,n_t}(k);\ k=0\sim M-1,\ n_t=0\sim N_t-1,\ n_r=0\sim N_r-1\}$ is the channel gain estimated by Eq. (18).

After the subcarrier de-mapping, one-tap MMSE-FDE is carried out as

$$[\tilde{\mathbf{R}}_0(k),...,\tilde{\mathbf{R}}_{Q-1}(k)]=\mathbf{W}^H(k)[\hat{\mathbf{R}}_0(k),...,\hat{\mathbf{R}}_{Q-1}(k)], \tag{24}$$

where $\tilde{\mathbf{R}}_q(k)=[\tilde{R}_{q,0}(k),...,\tilde{R}_{q,n_t-1},...,\tilde{R}_{q,N_t-1}(k)]^T$ and $\hat{\mathbf{R}}_q(k)=[\hat{R}_{q,0}(k),...,\hat{R}_{q,n_r-1}(k),...,\hat{R}_{q,N_r-1}(k)]^T$ for $q=0\sim Q-1$ with $[.]^H$ denoting the Hermitian transpose operation, respectively. $\mathbf{W}(k)=[\mathbf{W}_0(k),...,\mathbf{W}_{n_r}(k),...,\mathbf{W}_{N_r-1}(k)]^T$ with $\mathbf{W}_{n_r}(k)=[W_{n_r,0}(k),...,W_{n_r,n_t}(k),...,W_{n_r,N_t-1}(k)]$ is an $N_r\times N_t$ MMSE-FDE weight matrix. $W_{n_r,n_t}(k)$ is given by [13]

$$W_{n_r,n_t}(k)=\frac{\hat{H}_{n_r,n_t}(k)}{\frac{1}{N_t}\sum_{n_r=0}^{N_r-1}\sum_{n_t=0}^{N_t-1}\left|\hat{H}_{n_r,n_t}(k)\right|^2+\Gamma^{-1}}. \tag{25}$$

In Eq. (25), $\Gamma = PT_s / N_0$ is the average received SNR estimated by Eq. (19).

Next, STBC decoding is applied to demodulate M-subcarrier blocks of original signal as below. The k-th subcarrier group is expressed as demodulated subcarrier vector $\tilde{\mathbf{S}}_{N_t}(k) = [\tilde{S}_0(k), ..., \tilde{S}_{J-1}(k)]^T$ for k=0~M−1. $\tilde{\mathbf{S}}_{N_t}(k)$ is given as [9]-[10]

$$\tilde{\mathbf{S}}_{N_t=1}(k) = \tilde{R}_{0,0}(k), \tag{26.a}$$

$$\tilde{\mathbf{S}}_{N_t=2}(k) = \begin{bmatrix} \tilde{R}_{0,0}(k) + \tilde{R}^*_{1,1}(k) \\ \tilde{R}_{0,1}(k) - \tilde{R}^*_{1,0}(k) \end{bmatrix}, \tag{26.b}$$

$$\tilde{\mathbf{S}}_{N_t=3}(k) = \begin{bmatrix} \tilde{R}_{0,0}(k) + \tilde{R}^*_{1,1}(k) + \tilde{R}^*_{2,2}(k) \\ \tilde{R}_{0,1}(k) - \tilde{R}^*_{1,0}(k) + \tilde{R}^*_{3,2}(k) \\ \tilde{R}_{0,2}(k) - \tilde{R}^*_{2,0}(k) - \tilde{R}^*_{3,1}(k) \end{bmatrix}, \tag{26.c}$$

$$\tilde{\mathbf{S}}_{N_t=4}(k) = \begin{bmatrix} \tilde{R}_{0,0}(k) + \tilde{R}^*_{1,1}(k) + \tilde{R}^*_{2,2}(k) + \tilde{R}_{3,3}(k) \\ \tilde{R}_{0,1}(k) - \tilde{R}^*_{1,0}(k) - \tilde{R}_{2,3}(k) + \tilde{R}^*_{3,2}(k) \\ \tilde{R}_{0,2}(k) + \tilde{R}_{1,3}(k) - \tilde{R}^*_{2,0}(k) - \tilde{R}^*_{3,1}(k) \end{bmatrix}. \tag{26.d}$$

After transforming the frequency-domain signal $\{\tilde{S}_j(k);\ k=0\sim M-1\}$ back into the time-domain signal block by M-point IDFT, only the real part of the time-domain signal $\{\tilde{s}_j(n);\ n=0\sim M-1,\ j=0\sim J-1\}$ is outputted as

$$\begin{aligned} \tilde{s}_j(n) &= \mathrm{Re}\left\{ \frac{1}{\sqrt{M}} \sum_{k=0}^{M-1} \tilde{S}_j(k) \exp\left(j2\pi n \frac{k}{M} \right) \right\} \\ &= s_j(n) + \mathrm{Re}\{ \mu_{\mathrm{ISI}}(n) + \mu_{\mathrm{noise}}(n) \}, \end{aligned} \tag{27}$$

where $\mu_{\mathrm{ISI}}(n)$ and $\mu_{\mathrm{noise}}(n)$ are residual signal distortion, and equivalent noise, respectively.

3. Computer Simulation Results

In order to evaluate transmission performance of analog SC-FDE using STTD combined with receive antenna diversity, we use NMSE criterion defined as

$$\mathrm{NMSE} \equiv \frac{\frac{1}{N} \sum_{n=0}^{N-1} |\tilde{s}(n) - s(n)|^2}{\frac{1}{N} \sum_{n=0}^{N-1} s^2(n)}, \tag{28}$$

where N is the total number of transmitted signal samples.

Table 1. Computer simulation condition

Signal transmission	Analog SC-FDE using STTD & Rx antenna diversity
Total no. of subcarriers	N_c = 8192
Time-domain block size	M = 64
No. of Tx/Rx antennas	(N_t, N_r) = (1,1)~(2,4)
Spectrum shaping filter	Ideal brick wall LPF
GI size	N_g = 16
Sampling rate	$1/T$ = 8 kHz
Mapping	Distributed
Pilot block	Chu-sequence
Pilot size	N_p = 256
Cyclic delay size	Δ = 32
Channel	Doubly selective Rayleigh fading
	L=16-path uniform power delay profile
FDE weight	MMSE
Channel estimation	CDP-CE
Fast AGC	Ideal

3.1. Computer Simulation Condition

The computer simulation condition is summarized in Table 1. We assume the bandwidth-limited (4 kHz) voice transmission. A sampling rate of 8 kHz for the original analog signal, a time-domain signal block with size of M = 64 samples, an adjacent subcarrier interval of 125 Hz, and a distributed subcarrier mapping over N_c = 8192 subcarriers are assumed. As a propagation channel, the doubly selective Rayleigh fading channel having an L=16-path uniform power delay profile is considered. The time delay of the l-th path is set to $\tau_{n_r,n_t,l} = l$ and the maximum time delay difference is less than GI size (i.e., $L-1 \le N_g$). We consider Chu-sequence [16] as the known pilot signal having block size of N_p = 256. A unit cyclic delay size of Δ = 32 is assumed. One cyclic delay pilot block is added to the beginning of each group of Q STBC-encoded signal blocks.

3.2. NMSE Performance

The impact of CDP-CE error on NMSE performance of analog SC-FDE using STTD combined with receive antenna diversity in case of normalized maximum Doppler frequency $f_D T_s = 0$ and 3×10^{-6} is shown in Figs. 6 and 7, respectively. The performance in case of ideal channel estimation is also plotted. It is shown that NMSE performance in case of adopting CDP-CE is similar to that in case of having perfect knowledge of CSI. Fig. 7 shows that when receiving terminal moves, performance degradation occurs due to a drop in tracking ability and the loss of orthogonality in STBC under the doubly selective Rayleigh fading channel.

In order to examine the impact of receiving terminal moving speed on CDP-CE, NMSE performance as a function of $f_D T_s$ at the average received SNR Γ = 20 dB is shown in Fig. 8. It is shown that NMSE performance in case of using CDP-CE is similar to that under the perfect knowledge of CSI as $f_D T_s < 10^{-6}$. As an application, analog SC-FDE using STTD combined with receive antenna diversity can be applied to the existing AM radio broadcasting with carrier frequency of f_c = 1 MHz and whole bandwidth of $1/T_s = 1$MHz. In that case, $f_D T_s = 10^{-6}$ is equivalent to high-speed movement of 1,080 km/h. In other words, CDP-CE keeps the NMSE performance similar to that under the perfect knowledge of CSI even in a very high mobility environment.

4. Conclusion

In this paper, we studied an impact of channel estimation error of CDP-CE under a doubly selective Rayleigh fading channel on our recently proposed analog SC-FDE using STTD combined with receive antenna diversity for an application of analog SC-FDE to, as an example, radio broadcasting. We showed that practical CDP-CE keeps the NMSE performance similar to that under the perfect knowledge of CSI even in a very high

mobility environment.

References

[1] Y. Kim, B. J. Jeong, J. Chung, C.-S. Hwang, J. S. Ryu, K.-H. Kim, and Y. J. Kim, "Beyond 3G; vision, requirements, and enabling technologies," IEEE Commun. Mag., vol.41, no.3, pp.120-124, March 2003.

[2] Y. Park and F. Adachi, *Enhanced radio access technologies for next generation mobile communication*, Springer, 2007.

[3] A. Goldsmith, *Wireless communications*, Cambridge University Press, 2005.

[4] T. H. Vo, S. Kumagai, T. Obara, and F. Adachi, "Analog single-carrier transmission with frequency-domain equalization," Proc. 19th Asia-Pacific Conference on Communication (APCC), pp.698-702, Aug. 2013.

[5] D. Falconer, S. L. Ariyavistakul, A. Benyamin-Seeyar, and B. Eidson, "Frequency domain equalization for single-carrier broadband wireless systems," IEEE Commun. Mag., vol.40, no.4, pp.58-66, April 2002.

[6] F. Adachi, H. Tomeba, and K. Takeda, "Frequency-domain equalization for broadband single-carrier multiple access," IEICE Trans. Commun., vol.E92-B, no.5, pp.1441-1456, May 2009.

[7] T. H. Vo, S. Kumagai, and F. Adachi, "Analog SC-FDE using space-time transmit diversity combined with receive antenna diversity," IEICE Tech. Rep. on Radio Commun. System, vol.113, no.456, RCS2013-341, pp.211-214, March 2014.

[8] T. Fujimori, K. Takeda, K. Ozaki, A. Nakajima and F. Adachi, "Channel estimation using cyclic delay pilot for SC-MIMO multiplexing," IEICE Trans. Commun., vol.E91-B, no.9, Sept. 2008.

[9] S. M. Alamouti, "A simple transmit diversity technique for wireless communications," IEEE J. Select. Areas. Commun., vol.16, no.8, pp.1451-1458, Oct. 1998.

[10] V. Tarokh, H. Jafarkhani, and A. R. Calderbank, "Space-time block codes from orthogonal designs," IEEE Trans. Inf. Theory, vol.45, no.5, pp.1456-1467, July 1999.

[11] K. Takeda, T. Itagaki, and F. Adachi, "Application of space-time transmit diversity to single-carrier transmission with frequency-domain equalization and receive antenna diversity in a frequency-selective fading channel," IEE Proc.-Commun., vol.151, no.6, pp.627-632, Dec. 2004.

[12] Y. Han, Z. Wang, L. Li, and Y. Zhao, "A fast automatic gain control scheme for IEEE 802.15.4 receiver," Proc. IET 2nd International Conference on Wireless, Mobile and Multimedia Networks (ICWMMN), pp.167-170, Oct. 2008.

[13] R. Matsukawa, T. Obara, and F. Adachi, "Frequency-domain space-time block coded single-carrier distributed antenna network," IEICE Commun. Express, vol.2, no.4, pp.141-147, April 2013.

[14] H. G. Myung, J. Lim, and D. J. Goodman, "Single carrier FDMA for uplink wireless transmission," IEEE Vehicular Technol. Mag., vol.1, no.3, pp.30-38, Sept. 2006.

[15] S. Yoshioka, S. Kumagai, T. Yamamoto, T. Obara, and F. Adachi, "Single-carrier STBC diversity using CDP-CE and linear inter/extra-polation in a doubly selective fading channel," Proc. IEEE 10th Vehicular Technology Society Asia Pacific Wireless Communication Symposium (APWCS), Aug. 2013.

[16] D. C. Chu, "Polyphase codes with good periodic correlation properties," IEEE Trans. Inf. Theory, vol.18, no.4, pp.531-532, July 1972.

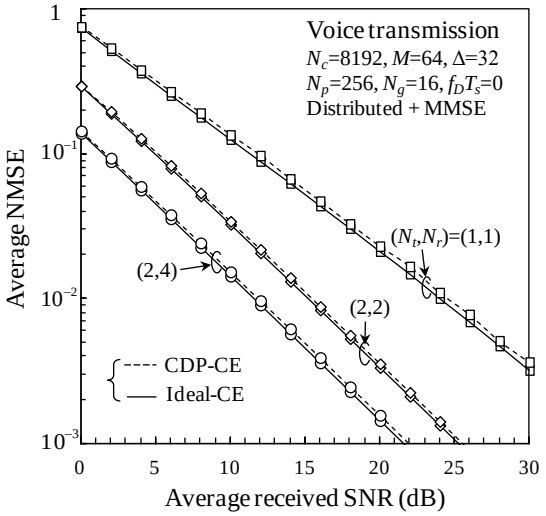

Fig. 6. NMSE performance in case of $f_DT_s = 0$.

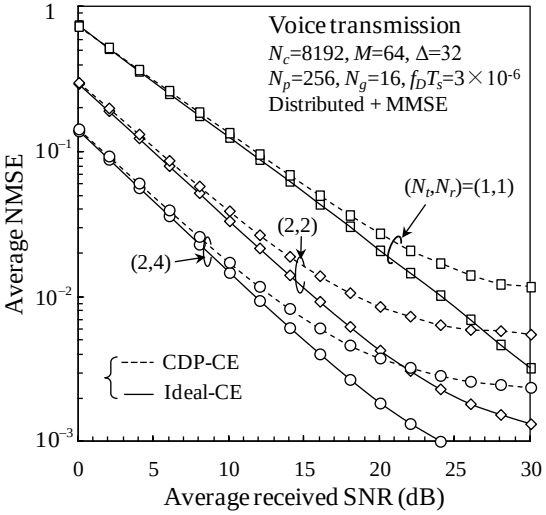

Fig. 7. NMSE performance in case of $f_DT_s = 3\times10^{-6}$.

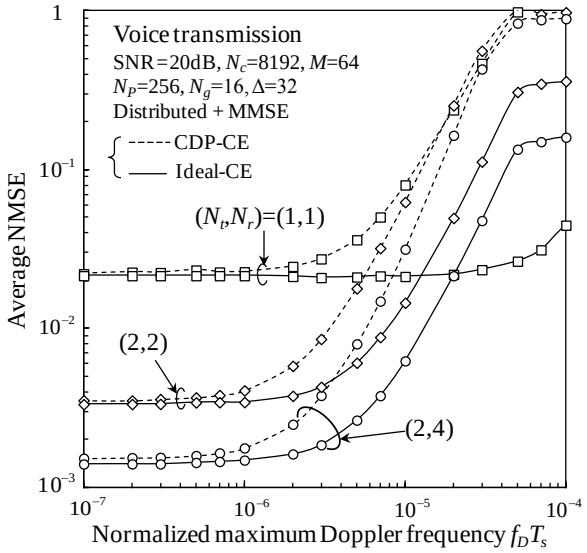

Fig. 8. NMSE performance under impact of f_DT_s when average received SNR Γ = 20 dB.